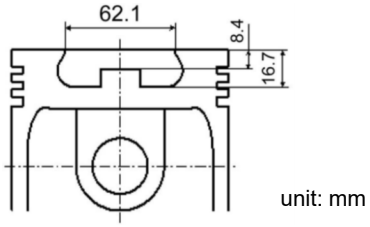

Figure 1 Cross section of the piston

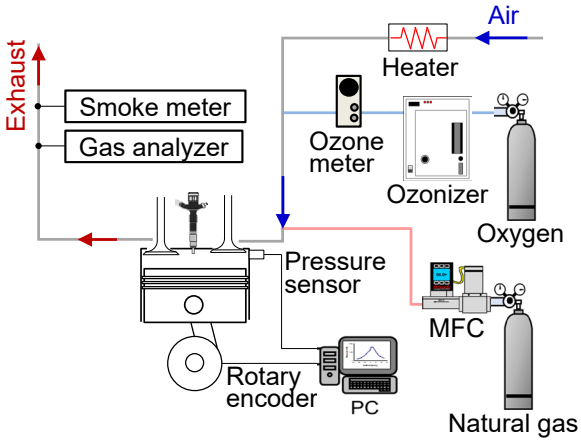

Figure 2 Schematic of the experimental setup with a single cylinder engine

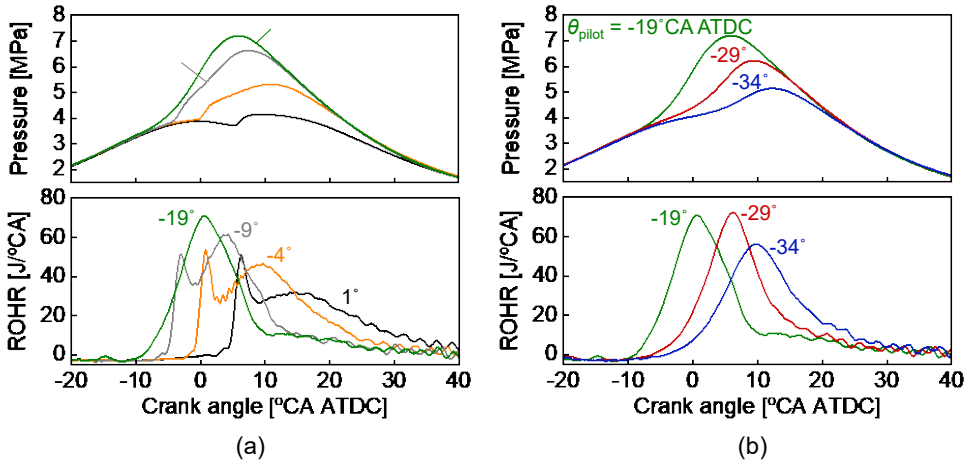

Figure 3 Changes in the profiles of the in-cylinder pressure and the rate of heat release (ROHR) with pilot injection timing of diesel fuel, θ_{pilot} (φ_{gas} = 0.42).
(a) θ_{pilot} = -19°, -9°, -4° and 1°CA ATDC; (b) θ_{pilot} = -34°, -29°, and -19°CA ATDC

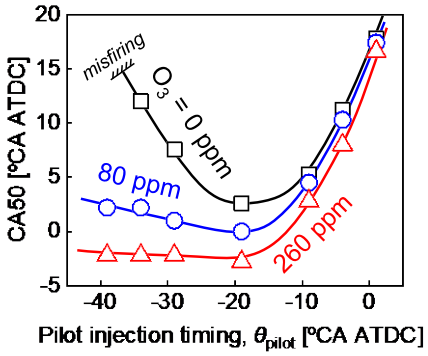

Figure 4 Effect of the ozone concentration on the fuel mass burned at 50% crank angle, CA50, at each pilot injection timing of the diesel fuel, θ_{pilot} (φ_{gas} = 0.42)

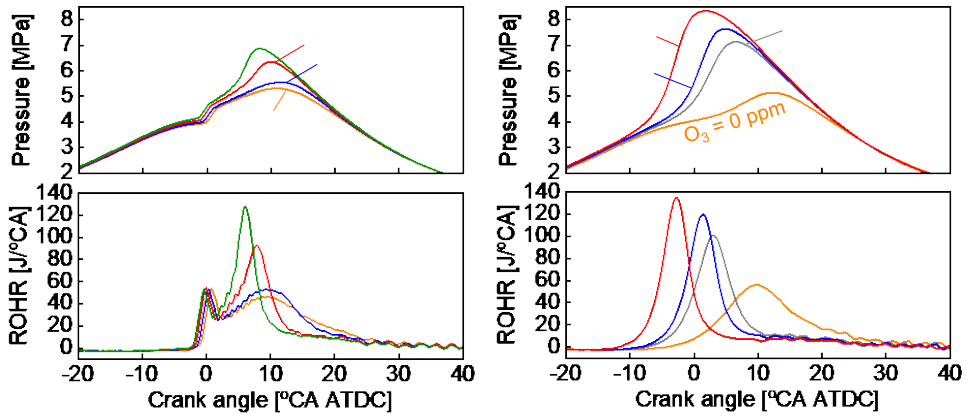

Figure 5 Changes in the profiles of the in-cylinder pressure and the rate of heat release (ROHR) with ozone concentration (φ_{gas} = 0.42).
(a) θ_{pilot} = -4˚ CA ATDC; (b) θ_{pilot} = -34˚CA ATDC

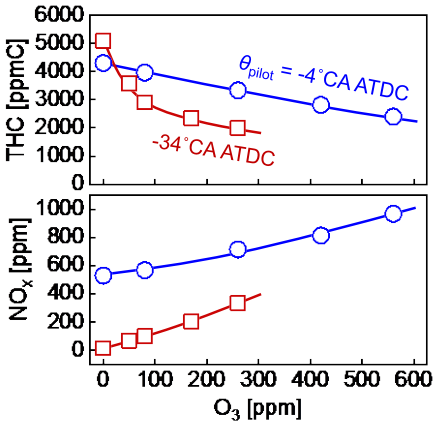

Figure 6 Comparison of the effects of the ozone addition on the THC and NO_x emissions between the pilot injection timings, θ_{pilot}, of -4˚CA ATDC and -34˚CA ATDC (φ_{gas} = 0.42)

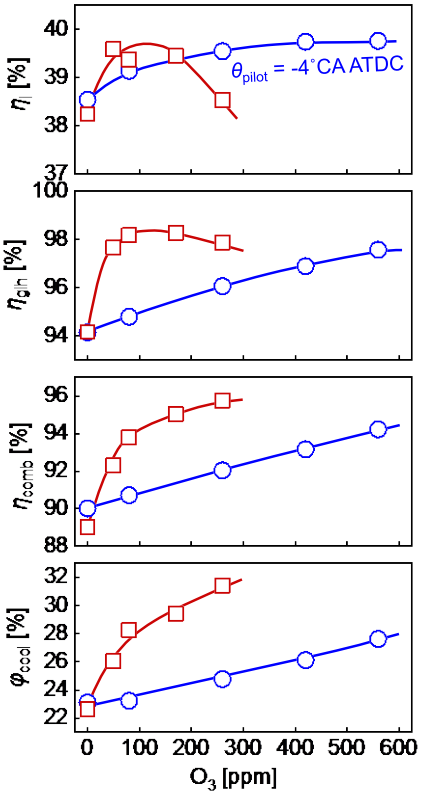

Figure 7 Comparison of the effects of the ozone addition on the indicated thermal efficiency, η_i, the degree of constant volume heat release, η_{glh}, the combustion efficiency, η_{comb}, and the cooling loss, φ_{cool}, between the pilot injection timings, θ_{pilot}, of -4˚CA ATDC and -34˚CA ATDC (φ_{gas} = 0.42)

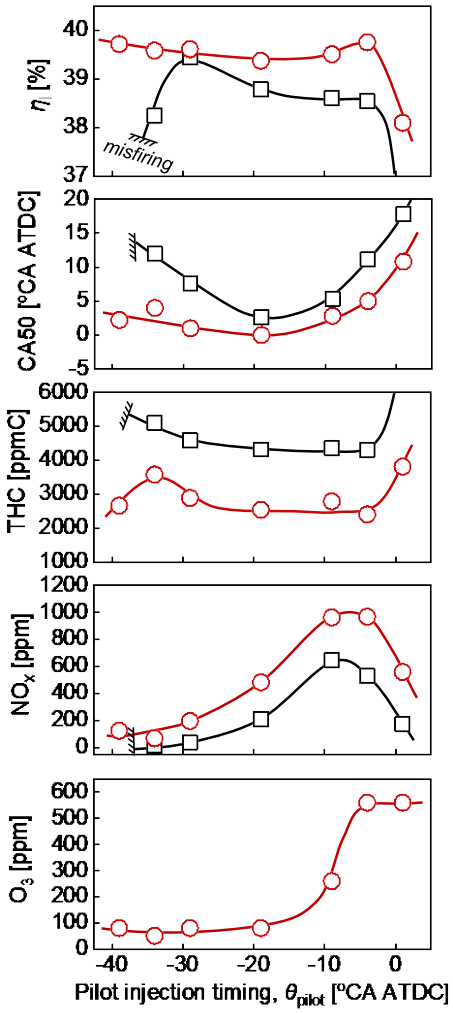

Figure 8 The indicated thermal efficiency, η_i, CA50, the THC and NO_x emissions, and the ozone concentration, at which the best η_i can be achieved.
The results without the ozone addition are shown for reference (φ_{gas} = 0.42).

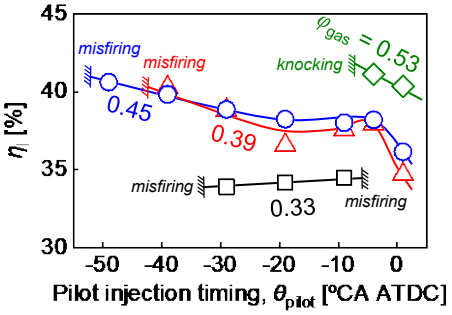

Figure 9 Comparison of the indicated thermal efficiency, η_i, among the equivalence ratios of the natural gas, φ_{gas} (without ozone)

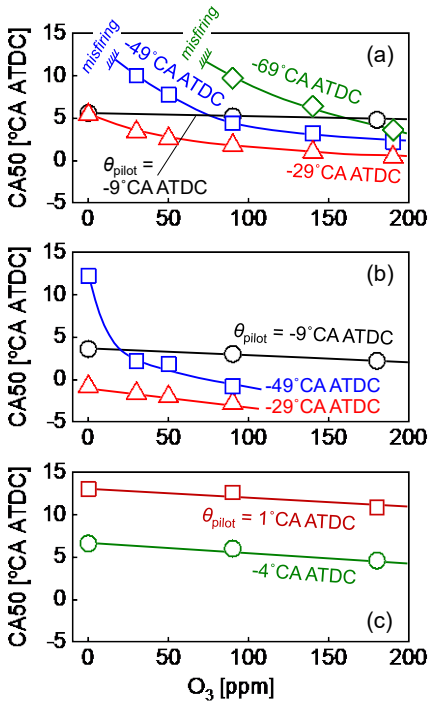

Figure 10 Effect of the ozone concentration on the fuel mass burned at the 50% crank angle, CA50, over the range of equivalence ratios of the natural gas, φ_{gas}
(a) φ_{gas} = 0.33; (b) φ_{gas} = 0.45; (c) φ_{gas} = 0.53

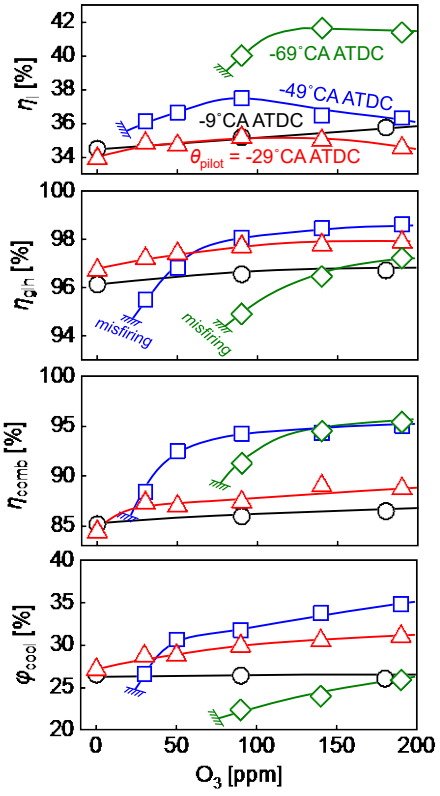

Figure 11 The indicated thermal efficiency, η_i, the degree of constant volume heat release, η_{glh}, the combustion efficiency, η_{comb}, and the cooling loss, φ_{cool}, at the various pilot injection timings, θ_{pilot} with the equivalence ratio of the natural gas, φ_{gas} of 0.33

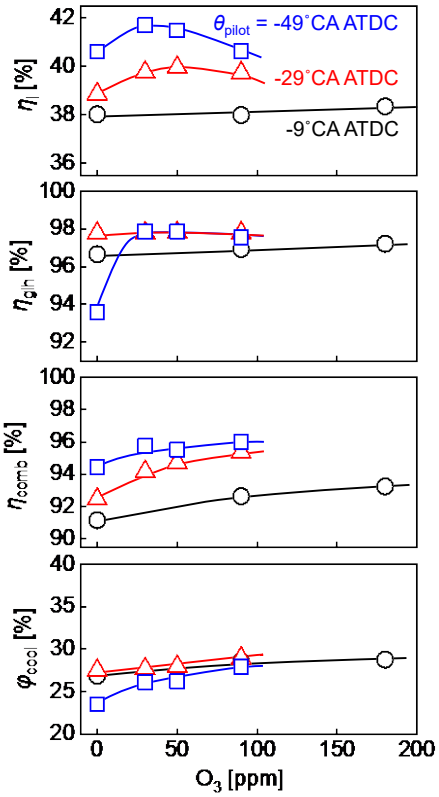

Figure 12 The indicated thermal efficiency, η_i, the degree of constant volume heat release, η_{glh}, the combustion efficiency, η_{comb}, and the cooling loss, φ_{cool}, at the various pilot injection timings, θ_{pilot} with the equivalence ratio of the natural gas, φ_{gas} of 0.45

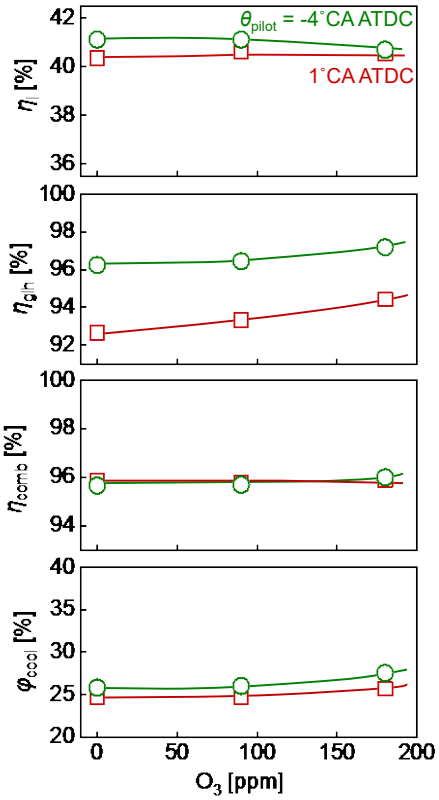

Figure 13 The indicated thermal efficiency, η_i, the degree of constant volume heat release, η_{glh}, the combustion efficiency, η_{comb}, and the cooling loss, φ_{cool}, at the various pilot injection timings, θ_{pilot} with the equivalence ratio of the natural gas, φ_{gas} of 0.53

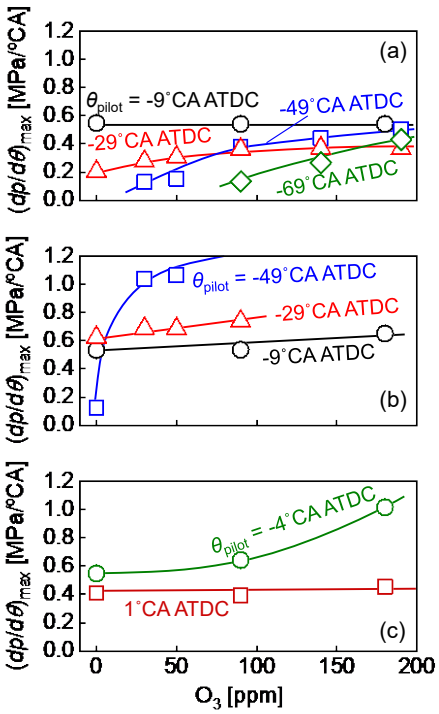

Figure 14 Effect of the ozone concentration on the maximum rate of pressure rise, $(dp/d\theta)_{max}$, over the range of equivalence ratios of the natural gas, φ_{gas}
(a) $\varphi_{gas} = 0.33$; (b) $\varphi_{gas} = 0.45$; (c) $\varphi_{gas} = 0.53$

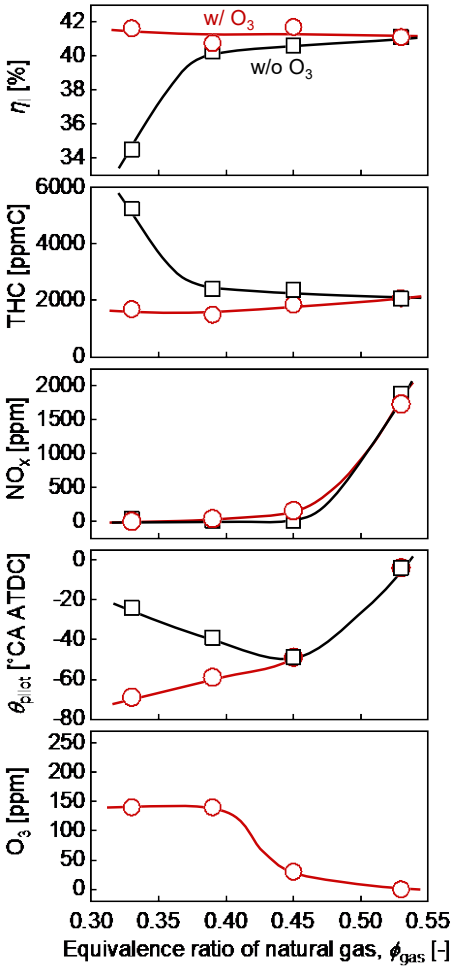

Figure 15 The indicated thermal efficiency, η_i, the THC and NO_x emissions, the pilot injection timing, θ_{pilot}, and the ozone (O_3) concentration at which the best η_i can be achieved over a range of equivalence ratios of the natural gas, φ_{gas}.

The results without the O_3 addition are shown for reference.

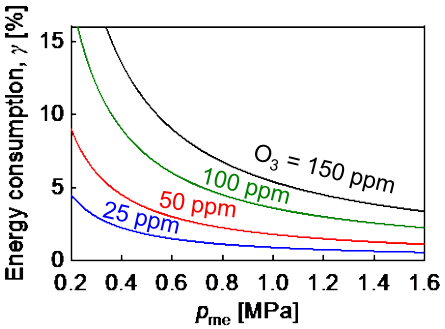

Fig.A-1 Ratio of the energy consumption caused by the ozone production, γ, versus the mean effective pressure, p_{me}